

# Demonstration of a spectrally scanned holographic Stokesmeter

Jong-Kwon Lee, John T. Shen \*, M.S. Shahriar

*Center for Photonic Communications and Computing, Department of Electrical Engineering and Computer Science, Northwestern University, 2145 N Sheridan Road, Evanston, IL 60208, USA*

Received 1 February 2007; accepted 2 May 2007

## Abstract

A holographic Stokesmeter (HSM) utilizes the inherent polarization sensitivity of volume gratings to determine all the Stokes parameters of input beams. A unique feature of the HSM is that it can be designed for spectral multiplexing at a high speed. Here, we report the demonstration of such a spectrally scanning HSM for two different wavelengths. Integration of such an HSM with a polarimetric imaging system will produce a device of potentially significant practical usage: a multi-spectral Stokes parameter camera (MSPC).

© 2007 Elsevier B.V. All rights reserved.

*Keywords:* Volume holography; Spectrally multiplexed gratings; Stokes parameters

Polarimetric imaging [1–3] can discriminate an object from its background by taking advantage of the fact that a given object emits and scatters light in a unique way depending on its polarimetric signature [4]. This polarimetric signature is dependent upon several characteristics of the target, including the roughness of the target surface and the shape and orientation of the target. On the other hand, the spectral signature of an object depends on properties such as surface coatings or chemical compositions. This specific combination of reflected and absorbed beams at varying wavelengths can be used to identify an object uniquely [5,6]. In general, polarization and multispectral imaging data are somewhat complementary because they depend on different optical characteristics of the object. Thus, it is in principle possible to perform contrast enhancement of a scene by using both polarization and spectral images of the scene. This type of imaging is potentially useful in applications such as target recognition, remote sensing, computer vision and scene discrimination [7–11].

Identifying the Stokes vector of a light field completely characterizes its polarization state. Current architectures

for such a Stokesmeter include mechanical quarter wave plate/linear polarizer systems, photo-detectors with polarization filtering gratings etched directly onto the pixel, and liquid crystal variable retarders [12–14]. While these architectures can be limited in speed or by the lack of an ability to determine the complete Stokes vector, a holographic Stokesmeter (HSM) [15] determines all the four Stokes parameters in parallel and at a high speed, limited primarily by the detector speed and the signal-to-noise ratio. Azzam and others [16,17] have proposed grating-based spectral Stokesmeters, but these devices are based upon thin gratings and the large spectral bandwidth of these gratings makes it difficult to implement a polarization imaging system [18].

The compact architecture of the HSM we proposed earlier, as shown in Fig. 1, consists of a pair of spatially separated gratings in a single substrate, two electro-optic modulators, and a single imaging system [19]. A pair of scanning mirrors are needed when the HSM is designed to perform spectrally multiplexed polarimetry.

We recall briefly [15,18,19] that the polarization imaging function can be analyzed using a set of Mueller matrices for each grating. The resulting measurement matrix relates the observed signals to the incident Stokes vector as follows:

\* Corresponding author. Tel.: +1 847 491 2797.

E-mail address: [jshen@ece.northwestern.edu](mailto:jshen@ece.northwestern.edu) (J.T. Shen).

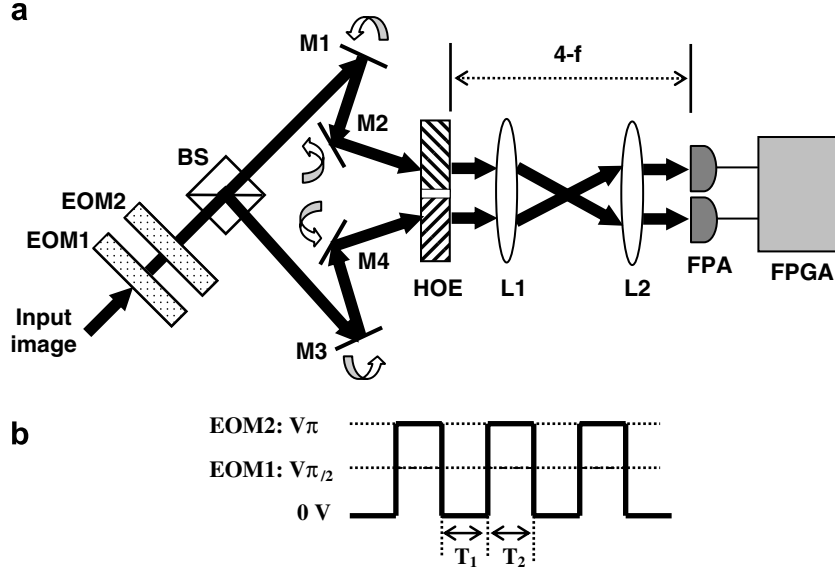


Fig. 1. (a) Polarimetric imaging system using two EOMs and a single Holographic substrate (b) input voltage signal scheme of two EOMs (EOM: electro-optic modulator, PBS: polarization beam splitter, HOE: holographic optical element, M: mirror, L: lens, FPA: focal plane array, FPGA: field programmable gate arrays).

$$\begin{bmatrix} I_{t1} \\ I_{t2} \\ I_{t3} \\ I_{t4} \end{bmatrix} = \begin{bmatrix} A_1 + B_1 & (A_1 - B_1) \cos(2\gamma_1) & (A_1 - B_1) \sin(2\gamma_1) & 0 \\ A_2 + B_2 & (A_2 - B_2) \cos(2\gamma_2) & (A_2 - B_2) \sin(2\gamma_2) & 0 \\ A_1 + B_1 & (A_1 - B_1) \cos(2\gamma_1) & 0 & -(A_1 - B_1) \sin(2\gamma_1) \\ A_2 + B_2 & (A_2 - B_2) \cos(2\gamma_2) & 0 & -(A_2 - B_2) \sin(2\gamma_2) \end{bmatrix} \begin{bmatrix} I \\ Q \\ U \\ V \end{bmatrix} \quad (1)$$

Here,  $(I, Q, U, V)$  represents the input Stokes parameters to be determined. These values are found by making measurements of the diffracted beams during two time periods as shown at the bottom of Fig. 1. During the interval  $T_1$ ,  $I_{t1}$  ( $I_{t2}$ ) are found from the diffracted intensity from the 1st (2nd) grating.  $I_{t3}$  ( $I_{t4}$ ) is the diffracted intensity from the 1st (2nd) grating during the interval  $T_2$ . The electro-optic modulators, active during  $T_2$ , serve to interchange the  $U$  and  $V$  parameters as described in reference [19].  $A_1, A_2$  ( $B_1, B_2$ ) characterize the diffraction efficiencies of the two gratings for s(p)-polarized input beams, taking into account the Fresnel reflections and transmissions at the interfaces. The angle  $\gamma_1$  ( $\gamma_2$ ) denotes the rotation of the substrate containing grating 1 (2). By measuring all four diffracted intensities from the holographic optical element (HOE) for each pixel of two focal plane arrays during interval  $T_1$  and  $T_2$ , we can construct the polarimetric image, by processing the signals with precalibrated field programmable gate arrays, for example.

The spectral resolving function of this design is achieved by multiplexing several gratings in each spatial location of the HOE. Each grating would be designed to produce a diffracted beam orthogonal to the substrate for a specific band of frequencies at a specific angle of incidence. Fig. 2a and b illustrate the geometry of such an HSM during the writing step. In this figure,  $n_1$  and  $n_2$  are the indices

of refraction outside and inside the substrate, respectively. For one of the gratings (Fig. 2a),  $2\theta_0$  is the angle between the two writing beams.  $2\theta'_0$  shows the corresponding angle inside the substrate. Similarly, for the other gratings (Fig. 2b),  $2\theta_1$  is the angle between the writing beams, and  $2\theta'_1$  is the corresponding angle inside the substrate. Both gratings are written with light field of a single color ( $\lambda_G$ ). From the Bragg condition for a thick hologram, the grating periods for the two gratings are given by

$$A_0 = \frac{\lambda_G}{2 \sin \theta'_0} = \frac{\lambda_G}{2 \sin \left( \frac{1}{2} \sin^{-1} \left( \frac{n_1}{n_2} \sin 2\theta_0 \right) \right)} \quad (2)$$

$$A_1 = \frac{\lambda_G}{2 \sin \theta'_1} = \frac{\lambda_G}{2 \sin \left[ \frac{1}{2} \sin^{-1} \left( \frac{n_1}{n_2} \sin(2\theta_1 + \delta) \right) - \frac{1}{2} \sin^{-1} \left( \frac{n_1}{n_2} \sin \delta \right) \right]} \quad (3)$$

In the reading step, an input beam at  $\lambda_G$  incident at angle  $2\theta_0$  will produce a diffracted beam perpendicular to the substrate for the first grating, as shown in Fig. 2c. For the second grating, to be read at a different wavelength ( $\lambda_R$ ), we can ensure that the diffracted beam will be perpendicular to the substrate by choosing the proper value of  $2\theta_1$  and  $\delta$ . The grating period of the second grating will have the following relations for two different wavelengths in order to satisfy the Bragg condition as shown in Fig. 2d:

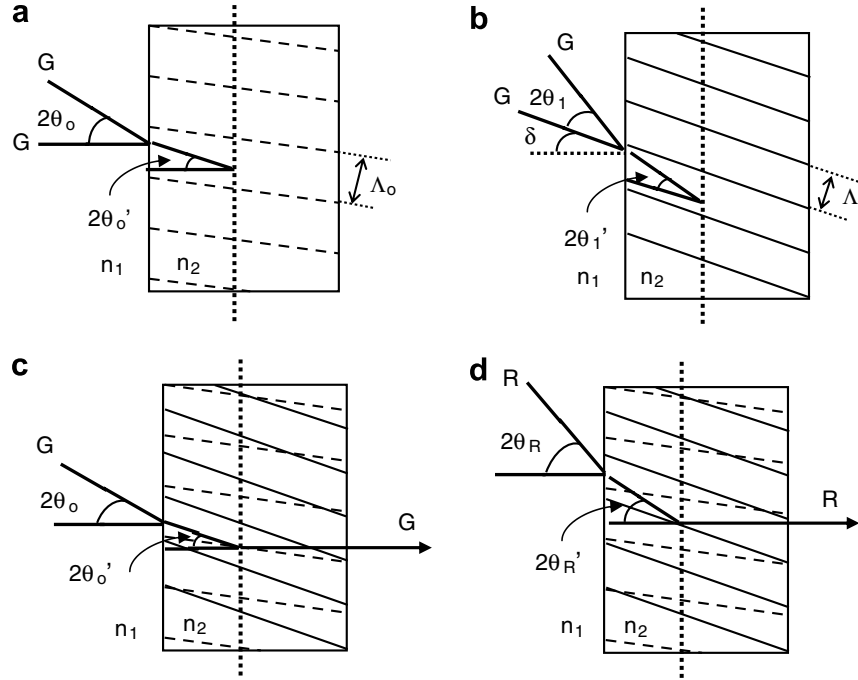


Fig. 2. (a) Writing condition with Nd–Yag laser beam (532 nm) for grating 1 (b) Writing condition with Nd–Yag laser beam (532 nm) for grating 2 (c) Reading condition with Nd–Yag laser beam (532 nm) for grating 1 (d) Reading condition with He–Ni laser beam (633 nm) for grating 2. ( $\Lambda_0$ ,  $\Lambda_1$ : the grating periods, G: Nd–Yag laser, R: He–Ni laser).

$$A_1 = \frac{\lambda_G}{2 \sin \theta'_1} = \frac{\lambda_R}{2 \sin \theta'_R} \quad (4)$$

or

$$\frac{\lambda_G}{2 \sin \left[ \frac{1}{2} \sin^{-1} \left( \frac{n_1}{n_2} \sin(2\theta_1 + \delta_1) \right) - \frac{1}{2} \sin^{-1} \left( \frac{n_1}{n_2} \sin \delta \right) \right]} = \frac{\lambda_R}{2 \sin \left[ \frac{1}{2} \sin^{-1} \left( \frac{n'_1}{n'_2} \sin 2\theta_R \right) \right]} \quad (5)$$

where  $n'_2$ ( $n'_1$ ) is the refractive index inside (outside) the substrate for the writing wavelength of  $\lambda_R$ . Therefore, an input beam at  $\lambda_R$  incident at angle  $2\theta_R$  for the 2nd grating

$$2\theta_R = \sin^{-1} \left( \frac{n'_2}{n'_1} \sin \left\{ 2 \sin^{-1} \left[ \frac{\lambda_R}{\lambda_G} \sin \left( \frac{1}{2} \sin^{-1} \left[ \frac{n_1}{n_2} \sin(2\theta_1 + \delta) \right] - \frac{1}{2} \sin^{-1} \left[ \frac{n_1}{n_2} \sin \delta \right] \right) \right\} \right) \quad (6)$$

will produce a diffracted beam orthogonal to the substrate. Using this method, we can create many angle-multiplexed gratings at the same location in a HOE of our compact device, where the maximum number of gratings would be limited by the  $M/\#$  of the material [20,21]. Thus, by scanning the angle of  $\theta_R$  without changing the location [22], it is possible to produce a spectrally resolved polarimetric image for a desired wavelength band. In principle, there can be as many wavelength bands as the  $M/\#$  [20,21] (which can be as high as 40 [23]). One can choose to write a number of gratings larger than the  $M/\#$  at the expense of the diffraction efficiency, which in turn will reduce the signal-to-noise ratio.

In order to demonstrate the feasibility of the spectrally multiplexed Stokesmeter, we wrote two angle-multiplexed gratings in both spatial positions of a 2 mm thick Memplex® [24] sample with a 532 nm frequency doubled Nd:YAG laser using the rotation angles of  $\gamma_1 = 0^\circ$  and  $\gamma_2 = 4^\circ$  for the substrate. To simplify the analysis, we chose the same writing angles of  $2\theta_0$  and  $2\theta_1 \sim 48^\circ$  for each grating, and a rotation angle of  $\delta \sim 5.1^\circ$  from Eq. (6) for the writing condition. By scanning the angle of incidence between  $48^\circ$  and  $58.2^\circ$  for wavelength of 532 nm and 633 nm, the output diffracted beams orthogonal to the HOE have been produced.

Fig. 3 shows the measured diffraction efficiencies from the two gratings in a thick hologram for two different

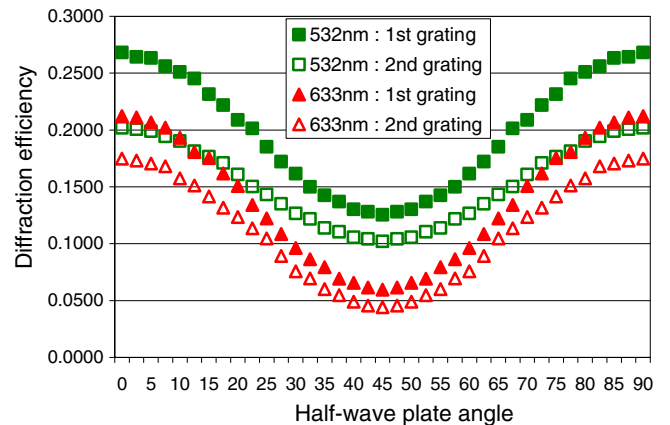


Fig. 3. Diffraction efficiencies vs. incident polarization of the two angle-multiplexed gratings, shown for four different contrast ratios (CR).

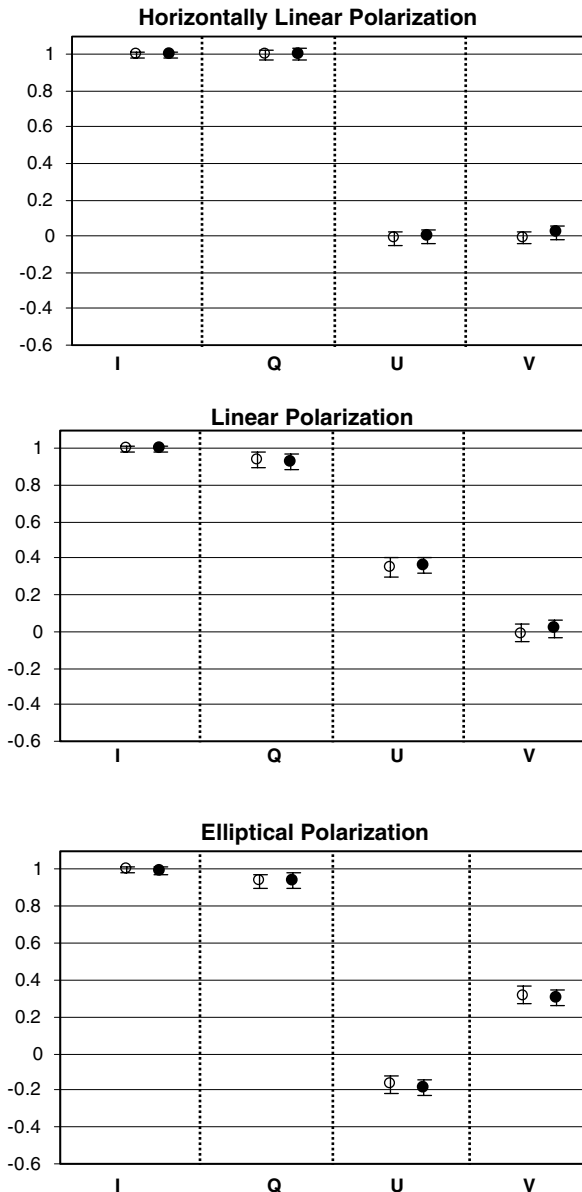


Fig. 4. The average values and the standard deviations of  $I$ ,  $Q$ ,  $U$  and  $V$  measured by the compact architecture of HSM for three different polarization states of the input beams (532 nm:  $\circ$ , 633 nm:  $\bullet$ ).

wavelengths of 532 nm and 633 nm. These diffraction efficiencies yield contrast ratios of 53.3% and 49.5% for 532 nm, and of 71.9% and 74.7% for 632 nm at two spatially separated locations. Based on this data, we can construct the measurement matrix of Eq. (1) for each wavelength. Here, we considered three different polarizations of the input beam: horizontal-linear  $[1, 1, 0, 0]$ , linear  $[1, 0.94, 0.35, 0]$ , and elliptical  $[1, 0.94, -0.17, 0.30]$ . Note that since operating speed is not an issue for this proof-of-principle demonstration, we have implemented the HSM by using a quarter wave plate and a half wave plate instead of a pair of EOMs, which are necessary only for high speed operation. Fig. 4 displays the measured average values

and the standard deviations of  $I$ ,  $Q$ ,  $U$  and  $V$  using this compact architecture for each wavelength (532 nm, 633 nm). The average values of the Stokes parameters for each wavelength are approximately equal to the actual values within the error range. This shows the feasibility of a spectrally multiplexed HSM in its compact architecture. One of the interesting applications for this device will be a multi-spectral Stokes parameter camera, which will consist of the spectrally scanning HSM in front of the imaging system, and be equipped with an FPGA based processor. The output of this camera will be four Stokes parameter images for any given spectral band.

In conclusion, we have demonstrated a spectrally scanned HSM, as a variation of the compact HSM developed earlier, by measuring arbitrary Stokes parameters of input beams for two different wavelengths. The ability to combine spectral discrimination with polarization imaging in a single device makes this HSM a unique device of significant interest: the multi-spectral Stokes parameter camera (MSPC). Such a device is expected to be of widespread practical utility.

## References

- [1] J.L. Pezzaniti, R.A. Chipman, *Opt. Eng.* 34 (1995) 1558.
- [2] K.P. Bishop, H.D. McIntire, M.P. Fetrow, L. McMackin, *Proc. SPIE* 3699 (1999) 49.
- [3] G.P. Nordin, J.T. Meier, P.C. Deguzman, M.W. Jones, *J. Opt. Soc. Am. A* 16 (1999) 1168.
- [4] A. Gerrard, J.M. Burch, *Introduction to Matrix Methods in Optics*, Dover Publications, NY, 1974.
- [5] Rene A.L. Tolboom, N.J. Dam, N.M. Sijtsma, *Opt. Lett.* 28 (2003) 21.
- [6] Marshall B. Long, C.F. Kaminski, K. Kohse-Hoinghaus, J.B. Jeffries, *Appl. Comb. Diag.* (2002).
- [7] W.G. Egan (Ed.), *Proc. SPIE* 1747 (1992) 154.
- [8] K.P. Bishop, H.D. McIntire, M.P. Fetrow, L. McMackin, *Proc. SPIE* 3699 (1999) 49.
- [9] L.J. Denes, M. Gottlieb, B. Kaminsky, D. Huber, *Proc. SPIE* 3240 (1998) 8.
- [10] T. Nee, S.F. Nee, *Proc. SPIE* 2469 (1995) 231.
- [11] P.J. Curran, *Remote Sens. Environ.* 12 (1982) 491.
- [12] D.H. Goldstein, *Appl. Opt.* 31 (1992) 6676.
- [13] J.L. Pezzaniti, R.A. Chipman, *Proc. SPIE* 2297 (1994) 468.
- [14] J.M. Bueno, P. Artal, *Opt. Lett.* 24 (1999) 64.
- [15] M.S. Shahriar, J.T. Shen, R. Tripathi, M. Kleinschmitt, T. Nee, S.F. Nee, *Opt. Lett.* 29 (2004) 298.
- [16] R.M.A. Azzam, K.A. Giardina, *J. Opt. Soc. Am. A* 10 (6) (1993) 1190.
- [17] T. Todorov, L. Nikolova, *Opt. Lett.* 17 (5) (1992) 358.
- [18] M.S. Shahriar, J.T. Shen, M.A. Hall, et al., *Opt. Commun.* 245 (6) (2005) 67.
- [19] J.-K. Lee, J.T. Shen, A. Heifetz, R. Tripathi, M.S. Shahriar, *Opt. Commun.* 259 (2) (2006).
- [20] H.N. Yum, P.R. Hemmer, R. Tripathi, J.T. Shen, M.S. Shahriar, *Opt. Lett.* 29 (2004) 15.
- [21] M.S. Shahriar, J. Riccobono, M. Kleinschmitt, J.T. Shen, et al., *Opt. Commun.* 220 (3) (2003) 75.
- [22] M.S. Shahriar, R. Tripathi, M. Kleinschmitt, J. Donghue, W. Weathers, M. Hug, J.T. Shen, *Opt. Lett.* 28 (2003) 7.
- [23] L. Dhar et al., *Opt. Lett.* 24 (7) (1999) 487.
- [24] D.N. Burzynski, S. Ghosal Kumar, D.R. Tyczka, U.S. Patent No. 6,344,297 (2002).